



ELSEVIER



Cancer Genetics 230 (2019) 13–20

Cancer
Genetics

ORIGINAL ARTICLE

Novel rearrangements involving the *RET* gene in papillary thyroid carcinoma

Julia Isabelle Staubitz^{a,*}, Arno Schad^b, Erik Springer^b, Krishnaraj Rajalingam^c, Hauke Lang^d, Wilfried Roth^b, Nils Hartmann^b, Thomas Johannes Musholt^a

^a Section of Endocrine Surgery, Department of General, Visceral and Transplantation Surgery, University Medical Center, Johannes Gutenberg University Mainz, Langenbeckstraße 1, D-55131 Mainz, Germany; ^b Institute of Pathology, University Medical Center, Johannes Gutenberg University Mainz, Langenbeckstraße 1, D-55131 Mainz, Germany; ^c Research Center for Immunotherapy, University Medical Center, Johannes Gutenberg University Mainz, Langenbeckstraße 1, D-55131 Mainz, Germany; ^d Department of General, Visceral and Transplantation Surgery, University Medical Center, Johannes Gutenberg University Mainz, Langenbeckstraße 1, D-55131 Mainz, Germany

Abstract

Background: In the field of gene fusions driving tumorigenesis in papillary thyroid carcinoma (PTC), rearrangement of the proto-oncogene *RET* is the most frequent alteration. Apart from the most common rearrangement of *RET* to *CCDC6*, more than 15 partner genes are yet reported. The landscape of *RET* rearrangements in PTC (“RET-PTC”) can notably be enlarged by modern targeted next-generation sequencing, indicating similarities between oncogenic pathways in other cancer types with identical genetic alterations.

Methods: Targeted next-generation sequencing was performed for two cases of *BRAF*-wild type PTC with confirmation of the results by Sanger sequencing. A “UniProt” database research was performed to assess protein alterations resulting from *RET* rearrangements.

Results: *RUFY2-RET* and *KIAA1468-RET* were detected. The fusion genes were not present in normal tissue of the index patients. The rearrangement *RUFY2-RET* lead to a fusion of the *RET* tyrosine kinase domain to a RUN domain and a coiled-coil domain. For *KIAA1468-RET*, a fusion to a LisH domain and two coiled-coil domains resulted.

Conclusions: *RUFY2-RET* and *KIAA1468-RET* are novel RET/PTC rearrangements. The fusions were previously described in non-small cell lung cancer. The rearrangement results in a fusion of the *RET* tyrosine kinase to regulatory domains of RUFY2 and KIAA1468.

Keywords RET/PTC, *RET* gene, RUFY2, KIAA1468, Papillary thyroid carcinoma.

© 2018 Elsevier Inc. All rights reserved.

Introduction

Differentiated thyroid carcinoma is a malignant tumor characterized by a high incidence. In the United States of America, from 1975 to 2014, the yearly incidence rose from 4.9 to 14.3 per 100,000 inhabitants [1,2]. Differentiated thyroid carcinoma usually is associated with a favorable outcome, following adequate surgical therapy. Still, up to 10% of carcinomas show recurrence and up to 30% develop distant

metastases [3]. Within the category of differentiated thyroid carcinoma, papillary thyroid carcinoma (PTC) is represented with a frequency of 80–85% [4]. In sporadic PTC, oncogenic fusions are present in 4–46%, involving *RET*, *BRAF*, *NTRK1*, *NTRK3*, *ALK*, *PPARG* and *THADA* [5–9]. Most gene fusions in PTC involve the *RET* (“rearranged during transfection”) gene [5,10–12]. The proto-oncogene *RET* encompasses 21 exons and is located on chromosome 10q11.21. It encodes a transmembrane receptor tyrosine kinase [13,14]. In most cases, the breakpoint within the *RET* gene is located in intron 11 [15–17]. The underlying pathological mechanism was reported as follows: a fusion to a promoter belonging to a gene, which is expressed in thyroid follicular cells, leads to an expression of *RET*, which otherwise remains clinically silent. A loss of the transmembrane region of *RET* is caused by its

Received August 28, 2018; received in revised form October 7, 2018; accepted November 7, 2018

* Corresponding author.

E-mail address: julia.staubitz@unimedizin-mainz.de

common rearrangements. The resulting cytosolic location of *RET*, and the fusion to dimerization motifs – usually coiled-coil regions – deriving from the fusion partner gene, lead to a constitutive activation of the encoded tyrosine kinase [18,19]. This unselected activation of the tyrosine kinase positively influences downstream pathways including RAS-MAPK and PI3K-AKT cascades, which are involved in the regulation of cell survival, proliferation, migration, and differentiation [18,20–23].

In PTC, *RET* fusion genes received the acronym RET/PTC, which were numbered consecutively [24]. Nowadays, due to the multiplicity of RET/PTC rearrangements, numerous authors prefer a nomenclature according to the genes involved [5]. 19 oncogenic *RET* rearrangements in PTC have yet been described, involving *AFAP1L2*, *AKAP13*, *CCDC6*, *ERC1*, *FKBP15*, *GOLGA5*, *HOOK3*, *KTN1*, *NCOA4*, *PCM1*, *PPFIBP2*, *PRKAR1A*, *RFG9*, *SPECC1L*, *TBL1XR*, *TRIM24*, *TRIM27*, *TRIM33* and *UEVLD* [5,25,26]. Of these, RET/PTC1 (*CCDC6-RET*) and RET/PTC3 (*NCOA4-RET*) were discovered to have the highest frequency (approximately 90% of all *RET* rearrangements). In sporadic PTC, the frequency of RET/PTC1 is 2 times higher than of RET/PTC3 [5,27–29].

Yet, it is uncertain, how many different rearrangements of the *RET* gene exist in papillary thyroid carcinoma, and whether different RET/PTC rearrangements lead to a variable course of disease. Modern next-generation sequencing methods are able to comprehensively reveal the identity and characteristics of RET/PTC fusion genes, which will notably enlarge the spectrum of the yet known *RET* rearrangements, offering the basis to address the question.

Material and methods

Patients and material

Tumor tissue was obtained from two patients who underwent surgery for papillary thyroid carcinoma at the University Medical Center Mainz. Routine histologic and molecular genetic assessment already excluded a BRAF-V600E mutation. The methods are described by Musholt et al. [30]. Absence of the BRAF mutation was confirmed in the present next-generation sequencing analysis.

The first tumor sample was obtained from index patient I, a 40-year-old female patient, who underwent total thyroidectomy and central lymph node dissection (level VI) with transcervical thymus resection for papillary thyroid carcinoma, follicular variant, pT2, pN1b (5/9), M0, R0 (Fig. 1(A)). Primary tumor was used for next-generation sequencing. Postoperatively, the patient was treated with radioactive iodine (RAI) therapy. In the last follow-up, four years after diagnosis, the patient was free of disease.

The second tumor sample was retrieved from index patient II, a 28 year-old male, who underwent secondary surgery at our hospital for the recurrence of PTC. The patient had previously undergone subtotal thyroidectomy with incomplete central lymph node dissection (pT3, pN1b (11/19), L1, V0, R0) and RAI therapy. After an interval of one year following primary surgery, a bilateral multifocal recurrence had been registered in scintigraphy and sonography, which is why he presented in our outpatient clinic. We performed a secondary cervical exploration with central lymph node dissection (level VI), transcervical thymus resection and selective lymph node

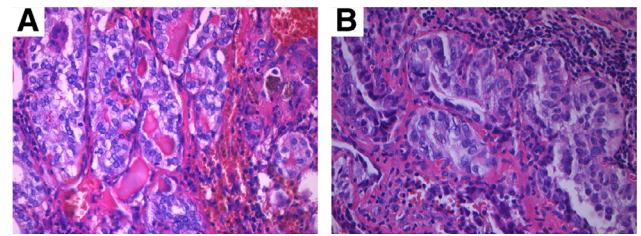


Fig. 1 Corresponding histologic slide of the specimen used for extraction of DNA and RNA. (A) Histology. Index patient I, harboring *RUFY2-RET*: follicular variant of papillary thyroid carcinoma with irregularly developed follicular structures, partly atrophic epithelium and condensed colloid. Tumor cells display pleomorphic, vacuolated and distorted nuclei. Formalin-fixed, paraffin-embedded tumor tissue, hematoxylin and eosin stain x400. (B) Index patient II, harboring *KIAA1468-RET*: lymphatic tissue with vast invasion of a classical papillary thyroid carcinoma. Pleomorphic, enlarged tumor cell nuclei are densely assembled. Formalin-fixed, paraffin-embedded tumor tissue, hematoxylin and eosin stain x400.

dissection of the lateral lymph node compartments. Thereby, a total of 32 lymph nodes was resected, of which 13 were affected by PTC, along with metastases in the perithyroidal tissue (Fig. 1(B)). Lymph node metastasis was used for next-generation sequencing. Until now, six months following secondary surgery, the patient is free of disease.

Main analysis: next-generation sequencing

Tumor tissue was retrieved from 4 µm formalin-fixed, paraffin-embedded (FFPE) tissue slices (80% tumor cells). Following manual microdissection, an extraction of DNA and RNA was performed using Maxwell RSC DNA and RNA FFPE Kits (Promega, Wisconsin, USA).

Anchored multiplex (AMP) polymerase chain reaction (PCR) based targeted next-generation sequencing was performed using Archer VariantPlex and Archer FusionPlex solid tumor kits (Archer, Boulder, Colorado, USA) according to the manufacturer's instructions. The panel allows for a simultaneous analysis of mutations and gene fusions in more than 60 genes, including e.g., *RET*, *NTRK1-3*, *ALK* and *RAS*. The technique allows for the detection and detailed analysis of genetic rearrangements by targeting one fusion partner involved. For VariantPlex, DNA libraries are created by two PCR reactions. The FusionPlex library preparation protocol includes the generation of cDNA from RNA template prior to PCR. In brief, each library is tagged with a unique combination of two adapter indices, which serve as molecular barcodes for sequencing. Sequencing was carried out using the MiSeq System (Illumina, San Diego, California, USA). Generated data was demultiplexed and aligned to the human reference genome hg19. The output (FASTQ format) was processed using "Archer Analysis" Software (Archer, Boulder, Colorado, USA).

For elimination of false positive results, filters for the detection of variants were set as follows: depth ≥ 100 ; allele frequency $\geq 10\%$. Inframe fusions were considered only. Called

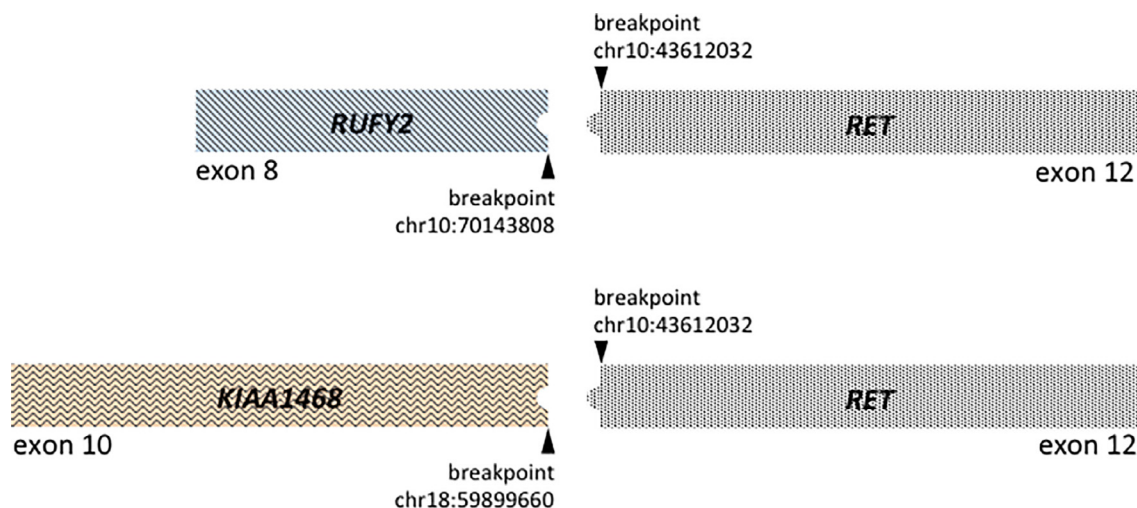


Fig. 2 Breakpoint on RNA level. *RUFY2-RET* and *KIAA1468-RET* fusion genes: breakpoint on RNA level is between *RET*, exon 12 (both cases), and exon 8 of *RUFY2* and exon 10 of *KIAA1468*, respectively. Results according to next-generation sequencing, “Archer Analysis” Software.

variants from the Cosmic (v65) scientific database were integrated by “Archer Analysis”.

Confirmation of results: RT-PCR and Sanger sequencing

To confirm the newly identified *RET/PTC* fusion genes *RUFY2-RET* and *KIAA1468-RET*, RNA deriving from tumor and normal thyroid/thymus tissue of the index patients underwent RT-PCR based fusion-specific amplification. cDNA was generated by reverse transcription polymerase chain reaction (RT-PCR) (annealing with random primers (C1181, Promega, Wisconsin, USA) at 70 °C; elongation at 40° for 60 min (mastermix: M-MLV Reverse Transcriptase M1701, Promega, Wisconsin, USA; RNasin Plus RNase inhibitor N2615, Promega, Wisconsin, USA; dNTP set 100 mM, Invitrogen, Thermo Fisher Scientific, Waltham, MA, USA)). For PCR amplification of *RUFY2-RET*, the following primers were used: *RUFY2_fw2*: ATGAAAACACAGCAGCACCT and *RET_rv2*: TGTACCCTGCTCTGCCTTTC (biomers.net GmbH, Ulm, Germany). For *KIAA1468-RET*, primers *RET_rv2*: TGTACCCTGCTCTGCCTTTC and *KIAA1468_fw2*: TGTCTCCTGCATTCCATCAA were applied. 2.5 µl of cDNA template were processed (program: 95° 5 min, 96° 5 s, 52° 5 min, 68° 7 s, 72° 1 min, 36 cycles, master mix: Qiagen Fast Cycling PCR Mix (Qiagen, Hilden, Germany). Sequence lengths of 145 bp (*RUFY2-RET*) and 288 bp (*KIAA1468-RET*) were calculated for the primer combinations. Gelectrophoresis (agarose gel 2%, peqGREEN) was performed.

In addition, the PCR products of the tumor samples underwent Sanger sequencing (GenomeLab DTCS Quick Start Kit (Beckman Coulter life sciences, Brea, USA), primers: *RET_Ex12_rv2*: TGTACCCTGCTCTGCCTTTC for *RUFY2-RET* and *KIAA1468_fw2*: TGTCTCCTGCATTCCATCAA for *KIAA1468-RET*, PCR program 96° 20 s, 50° 20 s, 60° 4 min, 30 cycles). Beckman Coulter CEQ8000 analyzer and software was used for analysis.

Prediction of protein expression

The common transcripts of the genes involved in *RET* rearrangements were retrieved from Ensembl platform (<http://ensemblgenomes.org>, [31]). Based on the results, full sequences of fusion genes were retraced. Translation to amino acid sequence was performed for original and fusion gene sequences using Expasy database (<https://www.expasy.org/>, [32]). For amino acid sequences, a “UniProt” (<https://www.uniprot.org>, [33]) database research was performed to identify the protein domains present in the original protein sequences, and newly identified fusion proteins *RUFY2-RET* and *KIAA1468-RET*.

Results

The tumors investigated were papillary thyroid carcinomas and derived from a 40-year old female (index patient I) and a 28 year-old male (index patient II). In the tumor tissue of index patient I, which belonged to the follicular subtype of PTC, *RUFY2-RET* was detected. The tissue of index patient II, the classical type of PTC, harbored *KIAA1468-RET*.

Using the Archer Variant and Fusion Plex Gene Panel (> 60 genes including e.g. *RET*, *NTRK1-3*, *ALK* and *RAS*), there were no other concomitant genetic variants to be detected in the present tumor samples.

Index patient I: *RUFY2-RET*

RUFY2-RET was detected with 144 Reads (%Reads: 73). Breakpoint of *RET* on RNA level was at the initial sequence of exon 12 (chr10:43612032). In *RUFY2*, it was in exon 8 (chr10:70143808). Fig. 2 depicts a schematic of the resulting hybrid oncogene with the breakpoint on RNA level.

Fusion gene-specific amplification following RT-PCR confirmed the existence of the newly described *RET/PTC* gene

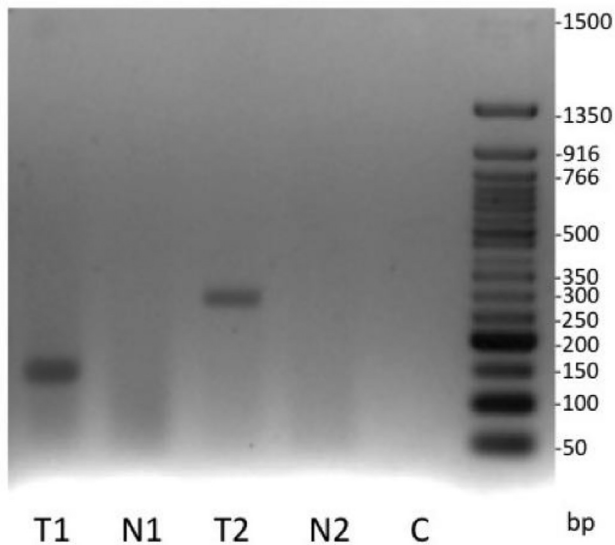


Fig. 3 Confirmation of *RUFY2-RET* and *KIAA1468-RET* by gel electrophoresis. Electrophoretic separation of PCR products, agarose gel: T1 = tumor of index patient I displaying *RUFY2-RET* fusion (145 bp). N1 = normal tissue (thyroid) without *RUFY2-RET* fusion of index patient I. T2 = tumor of index patient II displaying *KIAA1468-RET* fusion (288 bp). N2 = normal tissue (thymus) without *KIAA1468-RET* fusion of index patient II. C = control, H₂O (primer set: *RET_rv2* and *KIAA1468_fw2*).

fusion *RUFY2-RET* in the tumor tissue, whereas in normal thyroid tissue, it was not present (Fig. 3). Sanger sequencing of the PCR product of tumor tissue confirmed the breakpoint between *RUFY2* and *RET*, as described by “Archer Analysis” software (Fig. 2, Fig. 4).

According to the “UniProt” database research, *RUFY2* (*RUFY2-213* ENST00000602465.5, AF461266.1, Q8WXA3, 606 amino acids) contains a RUN domain at positions 37–169. Moreover, it harbors a coiled-coil region from positions 210–534 [33]. Whereas the RUN domain is expressed completely in *RUFY2-RET*, the coiled-coil region is partly represented in the fusion protein (positions 210–274). A zinc finger domain, located at positions 540–589 in *RUFY2*, is not expressed in *RUFY2-RET* [33], since the breakpoint to the *RET* proportion follows position 274 of *RUFY2*.

RUFY2-RET comprises 676 amino acids (Fig. 5). In *RUFY2-RET*, the aforementioned domains of *RUFY2* (RUN domain, coiled-coil domain) are connected to the tyrosine kinase region deriving from *RET* (positions 724–1016 in *RET*, *RET-202* ENST00000355710.7, P07949, 1114 amino acids). The transmembrane region of *RET* (positions 636–657) is not expressed in *RUFY2-RET*.

Positions in *RUFY2-RET* were exemplarily calculated using the following gene products: *RUFY2-213* ENST00000602465.5, AF461266.1, Q8WXA3, 606 amino acids and *RET-202* ENST00000355710.7, P07949, 1114 amino acids.

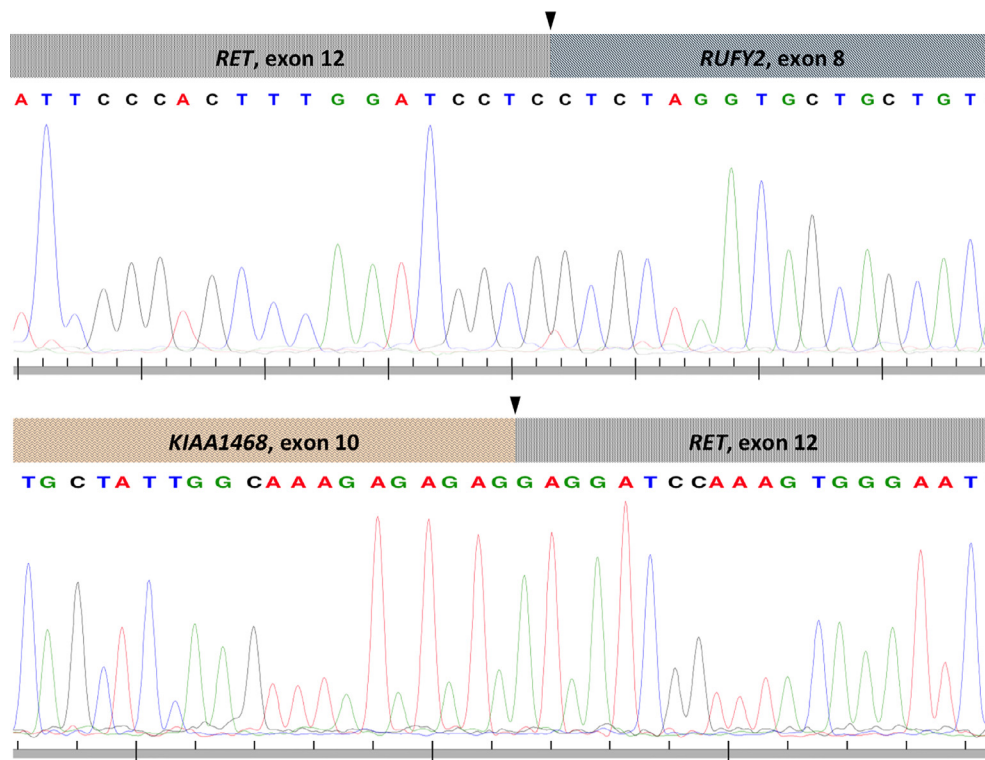


Fig. 4 Confirmation of *RUFY2-RET* and *KIAA1468-RET* by Sanger sequencing. Sanger sequencing confirmed the in-frame fusion between *RUFY2*-Exon 8 and *RET*-Exon 12 as well as between *KIAA1468*-Exon 10 and *RET*-Exon 12. In both cases the *RET* sequence is located at the 3'-end of the transcript. Note that Sanger sequencing was only performed in 3' to 5' direction for *KIAA1468-RET* fusion product, while the reverse complementary strand is shown for *RUFY2-RET* fusion transcript. Arrows indicate breakpoint.

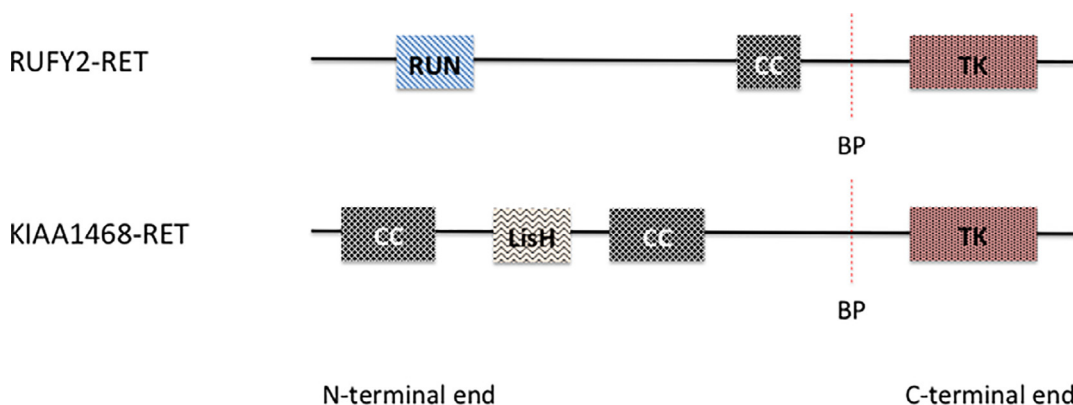


Fig. 5 Predicted functional domains of RUFY2-RET and KIAA1468-RET proteins. RUFY2-RET (676 amino acids) contains a RUN domain at positions 37–169, and partially a coiled-coil region from positions 210–274, which is connected to the tyrosine kinase region deriving from RET, positions 286–578. KIAA1468-RET (942 amino acids) contains a LisH domain (positions 255–287) and two coiled-coil regions (positions 197–231 and 359–397), which are connected to the tyrosine kinase region at positions 286–578. Positions according to “Uniprot” database analysis. CC = coiled-coil domain, LisH = LisH domain, RUN = RUN domain, TK = tyrosine kinase domain, BP = breakpoint.

Index patient II: *KIAA1468-RET*

KIAA1468-RET was registered with 104 Reads (%Reads: 80). Breakpoint of *RET* on RNA level was at the initial sequence in exon 12 (chr10:43612032). Breakpoint within *KIAA1468* was in exon 10 (chr18:59899660) (Fig. 1).

Fusion gene-specific amplification following RT-PCR confirmed the presence of the gene fusion *KIAA1468-RET* in the tumor tissue. In normal thymus tissue of the index patient, the fusion was not detectable (Fig. 3). Sanger sequencing of the PCR product of tumor tissue confirmed the breakpoint of the novel RET/PTC fusion on RNA level (Figs. 2 and 4).

In KIAA1468 (KIAA468-202, ENST00000398130.6, Q9P260 1216 amino acids), a LisH domain is located at positions 255–287 [33]. The LisH domain is included in the fusion protein KIAA1468-RET. There are 3 HEAT domains (HEAT1, HEAT2, HEAT3) at from positions 601–639, 640–679 and 1004–1042 in KIAA1468. However, these regions are not expressed in KIAA1468-RET, as the breakpoint to *RET* is located at positions 540. Yet, KIAA1468 contains two coiled-coil regions, encoded at positions 197–231 and 359–397, which are expressed by the fusion protein KIAA1468-RET. The fusion protein KIAA1468-RET (RET-202 ENST00000355710.7, P07949, 1114 amino acids) comprises 942 amino acids and couples the LisH domain and both coiled-coil domains to the *RET* tyrosine kinase domain (Fig. 5). Also KIAA1468-RET does not possess, as already described for RUFY2-RET, a transmembrane region, which is originally present in *RET*.

Positions in KIAA1468-RET were exemplarily calculated using the following gene products: KIAA468-202, ENST00000398130.6, Q9P260 1216 amino acids and RET-202 ENST00000355710.7, P07949, 1114 amino acids.

Discussion

New next-generation sequencing techniques, based on anchored multiplex PCR, allow for the detection of novel RET/PTC rearrangements. With singularly one fusion partner

gene within the panel of analysis, this technique facilitates the detection of genetic rearrangement, and the exact description of the previously unknown fusion partner gene. Sensitivity and specificity of rearrangement analysis with AMP-based next-generation sequencing, compared with reference assays, were shown to reach 100% [34]. Regarding *RET* rearrangements, this technique is more advantageous to the use of fluorescent in situ hybridization or to fusion-specific RT-PCR, as it combines a high sensitivity for detecting rearrangements and a high specificity by denominating the exact gene fusion - qualities, which the aforementioned techniques do not unite.

In the literature, for the two most common rearrangements of the *RET* gene, RET/PTC1 (*CCDC6-RET*) and RET/PRC3 (*NCOA4-RET*), the common breakpoints were described to be located within intron 11 [15,16]. In this RNA based analysis, the breakpoint resulted at the start of exon 12. This implies that on DNA level the common fragile site, intron 11, is involved.

The present findings demonstrate that *RUFY2-RET* and *KIAA1468-RET* are novel RET/PTC rearrangements. The existence of *RUFY2-RET* was already demonstrated in non-small cell lung cancer (NSCLC) using next-generation sequencing [34]. RUFY2 belongs to the RUFY protein family. The *RUFY2* gene encodes for the RUN and FYVE domain containing 2 proteins (also described as RABIP4R or ZFYVE13). It is located on chromosome 10q21.3. Within the RUFY2 protein, the N-terminal RUN domain is connected to a C-terminal FYVE zinc finger by a coiled-coil domain [33,35,36]. The RUN domain was reported to be involved in the regulation of cell polarity and membrane trafficking [37]. An expression of RUFY2 was registered by RNA-seq in normal human tissues primarily in brain, endometrium, ovary and thyroid [38].

The gene fusion KIAA1468-RET, newly discovered in PTC, contains a LisH domain located at positions 255–287 [33]. LisH regions can be involved in protein dimerization [39,40]. KIAA1468 also contains two coiled-coil regions, located at positions 197–231 and 359–397 of KIAA1468

(Fig. 5). KIAA1468-RET was previously observed in invasive mucinous adenocarcinoma of the lung [41].

Physiologically, *RET* activation is regulated by glial cell line-derived neurotrophic factor (GDNF)-family ligands, which, in presence of GDNF-family receptor- α proteins, can bind to the extracellular receptor domain of *RET*, leading to the formation of a dimer complex [18]. From this, an autophosphorylation of selected tyrosine residues at the intracellular kinase region of *RET* results. Depending on the phosphorylation site, different pathways are activated, including RAS-MAPK and PI3K-AKT cascades, which are involved in the regulation of cell survival, proliferation, migration, and differentiation [18,20,21].

Also, coiled-coil domains can facilitate oligo- and dimerization [42,43]. For different RET/PTC fusion proteins, including the most common one *CCDC6-RET* (RET/PTC1), an activation of the tyrosine kinase by protein dimerization via coiled-coil domains was reported in the literature [18,19]. As a coiled-coil domain is partially expressed in the novel gene fusion *RUFY2-RET* (*RUFY2*, positions 210–274), a dimerization might result. For *KIAA1468-RET*, a dimerization mediated by the coiled-coil domains at positions 197–231 and 359–397 and the LisH domain at positions 255–287 of *KIAA1468* is possible. By a resulting constitutive activation of the *RET* tyrosine kinase, a pathological activation of subsequent signaling cascades with oncogenic relevance appears plausible.

In addition to this, coiled-coil domains were reported to act as molecular spacers influencing kinase function [44]. By regulating the spatial relation between enzyme and substrate, for Rho kinases, a reformative way of kinase activation was demonstrated to be achieved by coiled-coil domains [45]. A potential regulation for the *RET* tyrosine kinase is possible in case of the fusion protein *RUFY2-RET* and *KIAA1468-RET*. Following this principle, in *KIAA1468-RET*, different processes than in *RUFY2-RET* could be propelled. For further investigation, larger cohorts of patient samples harboring the specific rearrangements, or artificially created thyrocyte cell lines, are possible models for elucidation.

Thus, the yet large variety of RET/PTC rearrangements (> 20 different fusion genes) should be analyzed with regard to differential activation of subsequent signaling cascades. Whereas a basic dimerization should consequently lead to a similar kinase activation pattern, and similar courses of disease, a specific condition, e.g., by differential kinase regulation potentially caused by alteration of the spatial relation between enzyme and substrate, might influence distinct pathways. Variable courses of disease would be the consequence. In the present case, the 28-year-old patient harboring *KIAA1468-RET* initially presented with lymph node metastases (pN1b), and an early recurrence after an extensive operative resection and RAI therapy was registered. The patient harboring *RUFY2-RET* was already 40 years of age at diagnosis. She also harbored lymph node metastases (pN1b). Following an adequate surgical resection and RAI therapy, no recurrence was registered in this case. In the patient harboring *RUFY2-RET*, the follicular variant of PTC was diagnosed (Fig. 1). For *RET* rearrangements, a potential role favoring the development of lymph node metastases was discussed in the literature [30,46,47]. A large-scale analysis of the clinical parameters as the development of lymph node metastases, recurrence, survival and histological subtype of PTC – in correlation with results from next-generation sequencing – could

contribute to the understanding, whether different RET/PTC rearrangements are associated with more or less aggressive features. Moreover, the group of *RET* rearrangement positive tumors should be compared to different PTC subgroups, as defined by e.g., *BRAF* mutation. For the invasive form of follicular variant of PTC, *BRAF* mutations were described to be present with a relatively high frequency compared to the encapsulated variant, in which RAS mutations prevail [48]. Even though analyses of larger cohorts support that RAS mutations are primarily present in the encapsulated, and therefore less aggressive form of the follicular variant of PTC [48,49], there are yet cases of particularly aggressive disease reported, as an isolated *NRAS* q61K mutation [50]. In the present sample, neither a *BRAF* mutation, nor any other genetic variant other than *RUFY2-RET*, was present. To prove clinical significance of the finding of *RUFY2-RET* in the follicular variant of PTC, an analysis of a larger cohort would be required.

The analysis of normal tissue (thyroid/thymus) of the index patients harboring *RUFY2-RET* and *KIAA1468-RET* did not show the specific rearrangement discovered in the tumor, which underlines the oncogenic relevance of the gene fusions. Moreover, the gene fusions *RUFY2-RET* and *KIAA1468-RET* were previously described in NSCLC [34,41]. Rearrangements involving the *RET* gene are observed in 1–2% of NSCLC. A notably higher prevalence in pre-selected cohorts without *EGFR*, *ALK* or *KRAS* mutations, the prevalence was reported to reach 16% [51–54]. The existence of *RET* rearrangements in NSCLC was found to be associated with more poorly differentiated tumors, and an earlier onset than in *EGFR*-mutant tumors [55].

In lung cancer harboring *RET* rearrangement, targeting the tyrosine kinase by inhibitors, as cabozantinib, vandetanib and sunitinib, is a possible treatment option, which in multicenter analysis led to complete or partial responses in up to 37% [56].

Currently, for advanced, RAI-refractory differentiated thyroid carcinoma, treatment with tyrosine kinase inhibitors so-rafenib and levatinib presents an option [57,58]. In addition to surgery and RAI therapy, also possible treatment approaches for NSCLC using additional tyrosine kinase inhibitors might be beneficial in patients suffering from PTC.

This research gives further evidence that multiple, different *RET* rearrangements are present in different subtypes of papillary thyroid carcinoma (classical papillary thyroid carcinoma, follicular variant of papillary thyroid carcinoma). To prove epidemiological significance of the findings, further research in larger cohorts are required. With the results as a basis, correlation with clinical course and treatment response to radioiodine therapy and tyrosine kinase inhibitors can further elucidate the issue, and give an important structure to the existing therapy algorithms.

Funding

This work was supported by the University Medical Center of the Johannes Gutenberg University Mainz.

Declarations of interest

None

Supplementary materials

Supplementary material associated with this article can be found, in the online version, at doi:[10.1016/j.cancer.2018.11.002](https://doi.org/10.1016/j.cancer.2018.11.002).

References

- [1] Haugen BR, Alexander EK, Bible KC, Doherty GM, Mandel SJ, Nikiforov YE, et al. 2015 American thyroid association management guidelines for adult patients with thyroid nodules and differentiated thyroid cancer: the American thyroid association guidelines task force on thyroid nodules and differentiated thyroid cancer. *Thyroid* 2016;26:1–133.
- [2] Davies L, Welch HG. Current thyroid cancer trends in the United States. *JAMA Otolaryngol Head Neck Surg* 2014;140:317–22.
- [3] Cooper DS, Doherty GM, Haugen BR, Kloos RT, Lee SL, Mandel SJ, et al. Revised American Thyroid Association management guidelines for patients with thyroid nodules and differentiated thyroid cancer. *Thyroid* 2009;19:1167–214.
- [4] Xing M. Molecular pathogenesis and mechanisms of thyroid cancer. *Nat Rev Cancer* 2013;13:184–99.
- [5] Yakushina VD, Lerner LV, Lavrov AV. Gene fusions in thyroid cancer. *Thyroid* 2018;28:158–67.
- [6] Agrawal N, Akbani R, Aksoy BA, Ally A, Arachchi H, Asa SL, et al. Integrated genomic characterization of papillary thyroid carcinoma. *Cell* 2014;159:676–90.
- [7] Prasad ML, Vyas M, Horne MJ, Virk RK, Morotti R, Liu Z, et al. NTRK fusion oncogenes in pediatric papillary thyroid carcinoma in northeast United States. *Cancer* 2016;122:1097–107.
- [8] Lu Z, Zhang Y, Feng D, Sheng J, Yang W, Liu B. Targeted next generation sequencing identifies somatic mutations and gene fusions in papillary thyroid carcinoma. *Oncotarget* 2017;8:45784–92.
- [9] Zehir A, Benayed R, Shah RH, Syed A, Middha S, Kim HR, et al. Mutational landscape of metastatic cancer revealed from prospective clinical sequencing of 10,000 patients. *Nat Med* 2017;23:703–13.
- [10] Fenton CL, Lukes Y, Nicholson D, Dinauer CA, Francis GL, Tuttle RM. The *ret*/PTC mutations are common in sporadic papillary thyroid carcinoma of children and young adults. *J Clin Endocrinol Metab* 2000;85:1170–5.
- [11] Liu RT, Chou FF, Wang CH, Lin CL, Chao FP, Chung JC, et al. Low prevalence of *RET* rearrangements (*RET*/*PTC1*, *RET*/*PTC2*, *RET*/*PTC3*, and *ELKS-RET*) in sporadic papillary thyroid carcinomas in Taiwan Chinese. *Thyroid* 2005;15:326–35.
- [12] Guerra A, Sapio MR, Marotta V, Campanile E, Moretti MI, Deandra M, et al. Prevalence of *RET*/*PTC* rearrangement in benign and malignant thyroid nodules and its clinical application. *Endocr J* 2011;58:31–8.
- [13] Ishizaka Y, Itoh F, Tahira T, Ikeda I, Sugimura T, Tucker J, et al. Human *ret* proto-oncogene mapped to chromosome 10q11.2. *Oncogene* 1989;4:1519–21.
- [14] Takahashi M, Ritz J, Cooper GM. Activation of a novel human transforming gene, *ret*, by DNA rearrangement. *Cell* 1985;42:581–8.
- [15] Nikiforov YE, Koshoffer A, Nikiforova M, Stringer J, Fagin JA. Chromosomal breakpoint positions suggest a direct role for radiation in inducing illegitimate recombination between the *ELE1* and *RET* genes in radiation-induced thyroid carcinomas. *Oncogene* 1999;18:6330–4.
- [16] Smanik PA, Furminger TL, Mazzaferri EL, Jhiang SM. Breakpoint characterization of the *ret*/*PTC* oncogene in human papillary thyroid carcinoma. *Hum Mol Genet* 1995;4:2313–18.
- [17] Gandhi M, Dillon LW, Pramanik S, Nikiforov YE, Wang YH. DNA breaks at fragile sites generate oncogenic *RET*/*PTC* rearrangements in human thyroid cells. *Oncogene* 2010;29:2272–2280.
- [18] Arighi E, Borrello MG, Sariola H. *RET* tyrosine kinase signaling in development and cancer. *Cytokine Growth Factor Rev* 2005;16:441–67.
- [19] Santoro M, Melillo RM, Carlomagno F, Fusco A, Vecchio G. Molecular mechanisms of *RET* activation in human cancer. *Ann N York Acad Sci* 2002;963:116–21.
- [20] Santoro M, Carlomagno F. Central role of *RET* in thyroid cancer. *Cold Spring Harb Perspect Biol* 2013;5.
- [21] Freche B, Guillaumot P, Charmetant J, Pelletier L, Luquain C, Christiansen D, et al. Inducible dimerization of *RET* reveals a specific AKT deregulation in oncogenic signaling. *J Biol Chem* 2005;280:36584–91.
- [22] Sariola H, Saarma M. Novel functions and signalling pathways for GDNF. *J Cell Sci* 2003;116:3855–62.
- [23] Encinas M, Crowder RJ, Milbrandt J, Johnson EM Jr. Tyrosine 981, a novel *ret* autophosphorylation site, binds c-Src to mediate neuronal survival. *J Biol Chem* 2004;279:18262–9.
- [24] Marotta V, Guerra A, Sapio MR, Vitale M. *RET*/*PTC* rearrangement in benign and malignant thyroid diseases: a clinical standpoint. *Eur J Endocrinol* 2011;165:499–507.
- [25] Hsiao SJ, Nikiforov YE. Molecular approaches to thyroid cancer diagnosis. *Endocr Relat Cancer* 2014;21:T301–13.
- [26] Yoo SK, Lee S, Kim SJ, Jee HG, Kim BA, Cho H, et al. Comprehensive analysis of the transcriptional and mutational landscape of follicular and papillary thyroid cancers. *PLoS Genet* 2016;12:e1006239.
- [27] Rabes HM, Demidchik EP, Sidorow JD, Lengfelder E, Beimefroh C, Hoelzel D, et al. Pattern of radiation-induced *RET* and *NTRK1* rearrangements in 191 post-chernobyl papillary thyroid carcinomas: biological, phenotypic, and clinical implications. *Clin Cancer Res* 2000;6:1093–103.
- [28] Santoro M, Thomas GA, Vecchio G, Williams GH, Fusco A, Chiappetta G, et al. Gene rearrangement and chernobyl related thyroid cancers. *Br J Cancer* 2000;82:315–22.
- [29] Klugbauer S, Demidchik EP, Lengfelder E, Rabes HM. Molecular analysis of new subtypes of *ELE*/*RET* rearrangements, their reciprocal transcripts and breakpoints in papillary thyroid carcinomas of children after Chernobyl. *Oncogene* 1998;16:671–5.
- [30] Musholt TJ, Schonefeld S, Schwarz CH, Watzka FM, Musholt PB, Fottner C, et al. Impact of pathognomonic genetic alterations on the prognosis of papillary thyroid carcinoma. *ESES vienna presentation. Langenbecks Arch Surg* 2010;395:877–83.
- [31] Kersey PJ, Allen JE, Allot A, Barba M, Boddu S, Bolt BJ, et al. Ensembl genomes 2018: an integrated omics infrastructure for non-vertebrate species. *Nucl Acids Res* 2018;46:D802–D8d8.
- [32] Gasteiger E, Gattiker A, Hoogland C, Ivanyi I, Appel RD, Bairoch A. ExPASy: the proteomics server for in-depth protein knowledge and analysis. *Nucl Acids Res* 2003;31:3784–8.
- [33] The UniProt Consortium UniProt: the universal protein knowledgebase. *Nucl Acids Res* 2017;45:D158–DD69.
- [34] Zheng Z, Liebers M, Zhelyazkova B, Cao Y, Panditi D, Lynch KD, et al. Anchored multiplex PCR for targeted next-generation sequencing. *Nat Med* 2014;20:1479–84.
- [35] Yang J, Kim O, Wu J, Qiu Y. Interaction between tyrosine kinase Etk and a RUN domain- and FYVE domain-containing protein RUFY1. A possible role of ETK in regulation of vesicle trafficking. *J Biol Chem* 2002;277:30219–26.
- [36] Barbe L, Lundberg E, Oksvold P, Stenius A, Lewin E, Bjorling E, et al. Toward a confocal subcellular atlas of the human proteome. *Mol Cell Proteom* 2008;7:499–508.
- [37] Kitagishi Y, Matsuda S. RUFY, rab and rap family proteins involved in a regulation of cell polarity and membrane trafficking. *Int J Mol Sci* 2013;14:6487–98.

- [38] Fagerberg L, Hallstrom BM, Oksvold P, Kampf C, Djureinovic D, Odeberg J, et al. Analysis of the human tissue-specific expression by genome-wide integration of transcriptomics and antibody-based proteomics. *Mol Cell Proteom* 2014;13:397–406.
- [39] Mateja A, Cierpicki T, Paduch M, Derewenda ZS, Otlewski J. The dimerization mechanism of LIS1 and its implication for proteins containing the LisH motif. *J Mol Biol* 2006;357:621–31.
- [40] Gerlitz G, Darhin E, Giorgio G, Franco B, Reiner O. Novel functional features of the Lis-H domain: role in protein dimerization, half-life and cellular localization. *Cell Cycle* 2005;4:1632–40.
- [41] Nakaoku T, Tsuta K, Ichikawa H, Shiraishi K, Sakamoto H, Enari M, et al. Druggable oncogene fusions in invasive mucinous lung adenocarcinoma. *Clin Cancer Res* 2014;20:3087–93.
- [42] Apgar JR. Predicting helix orientation for coiled-coil dimers. *2008*;72:1048–65.
- [43] Lu Q, Ye F, Wei Z, Wen Z, Zhang M. Antiparallel coiled-coil-mediated dimerization of myosin X. *Proc Natl Acad Sci* 2012;109:17388–93.
- [44] Truebestein L, Leonard TA. Coiled-coils: the long and short of it. *Bioessays* 2016;38:903–16.
- [45] Truebestein L, Elsner DJ, Fuchs E, Leonard TA. A molecular ruler regulates cytoskeletal remodelling by the Rho kinases. *Nat Commun* 2015;6.
- [46] Adeniran AJ, Zhu Z, Gandhi M, Steward DL, Fidler JP, Giordano TJ, et al. Correlation between genetic alterations and microscopic features, clinical manifestations, and prognostic characteristics of thyroid papillary carcinomas. *Am J Surg Pathol* 2006;30:216–22.
- [47] Romei C, Elisei R. RET/PTC translocations and clinico-pathological features in human papillary thyroid carcinoma. *Front Endocrinol (Lausanne)* 2012;3:54.
- [48] Rivera M, Ricarte-Filho J, Knauf J, Shaha A, Tuttle M, Fagin JA, et al. Molecular genotyping of papillary thyroid carcinoma follicular variant according to its histological subtypes (encapsulated vs infiltrative) reveals distinct BRAF and RAS mutation patterns. *Mod Pathol* 2010;23:1191–200.
- [49] Nikiforov YE, Seethala RR, Tallini G, Baloch ZW, Basolo F, Thompson LDR, et al. Nomenclature revision for encapsulated follicular variant of papillary thyroid carcinoma: a paradigm shift to reduce overtreatment of indolent tumors. *JAMA Oncol* 2016;2:1023–9.
- [50] Mehrzad R, Nishino M, Nucera C, Dias-Santagata D, Hennessey JV, Hasselgren PO. Invasive follicular variant of papillary thyroid cancer harboring the NRAS mutation Q61K and presenting with bone metastasis—a case report. *Int J Surg Case Rep* 2017;38:180–4.
- [51] Lipson D, Capelletti M, Yelensky R, Otto G, Parker A, Jarosz M, et al. Identification of new ALK and RET gene fusions from colorectal and lung cancer biopsies. *Nat Med* 2012;18:382–4.
- [52] Takeuchi K, Soda M, Togashi Y, Suzuki R, Sakata S, Hatano S, et al. RET, ROS1 and ALK fusions in lung cancer. *Nat Med* 2012;18:378–81.
- [53] Kohno T, Ichikawa H, Totoki Y, Yasuda K, Hiramoto M, Nanno T, et al. KIF5B-RET fusions in lung adenocarcinoma. *Nat Med* 2012;18:375–7.
- [54] Lee SE, Lee B, Hong M, Song JY, Jung K, Lira ME, et al. Comprehensive analysis of RET and ROS1 rearrangement in lung adenocarcinoma. *Mod Pathol* 2015;28:468–79.
- [55] Wang R, Hu H, Pan Y, Li Y, Ye T, Li C, et al. RET fusions define a unique molecular and clinicopathologic subtype of non-small-cell lung cancer. *J Clin Oncol* 2012;30:4352–9.
- [56] Gautschi O, Milia J, Filleron T, Wolf J, Carbone DP, Owen D, et al. Targeting RET in patients with RET-rearranged lung cancers: results from the global, multicenter RET registry. *J Clin Oncol* 2017;35:1403–10.
- [57] Brose MS, Nutting CM, Jarzab B, Elisei R, Siena S, Bastholt L, et al. Sorafenib in radioactive iodine-refractory, locally advanced or metastatic differentiated thyroid cancer: a randomised, double-blind, phase 3 trial. *Lancet* 2014;384:319–28.
- [58] Schlumberger M, Tahara M, Wirth LJ, Robinson B, Brose MS, Elisei R, et al. Lenvatinib versus placebo in radioiodine-refractory thyroid cancer. *N Engl J Med* 2015;372:621–30.